Pergamon

PII: S0301-9322(96)00051-1

Int. J. Multiphase Flow Vol. 23, No. 1, pp. 183–192, 1997

0301-9322/97 $17.00 + 0.00

PELLET DYNAMICS IN A GAS-FILLED VERTICAL COLUMN

A. N. KORNILOVSKY and A. A. HARMS
Department of Engineering Physics, McMaster University, Hamilton, Ontario, L8S 4L7, Canada

(Received 28 August 1995; in revised form 21 July 1996)

Abstract—The dynamics of pellets in a gas-filled vertical column are investigated by analytical methods and including considerations of molecular dynamics simulation. For some extremes of interest, we find effective formulations for generally intractable cases thereby allowing useful parametrization and numerical assessments. As a particular case, pellet mean residence times for a range of exit constrictions are assessed. Copyright © 1996 Elsevier Science Ltd.

Key Words: drag force approximation, free particle motion, pellet escape time, computational simulation

1. INTRODUCTION

The motion of particles in turbulent flows is a long-standing subject of interest with both experimental (e.g. Kaftori *et al.* 1995) and numerical (e.g. Datta and Dalal 1995; Pedinotti *et al.* 1992) advances continuing to be reported. A new important application of such phenomena has recently arisen in connection with the development of a fuel pellet suspension nuclear reactor which appears to offer deterministic avoidance of a core melt accident; in such reactors, the core consists of a set of vertical columns which are filled by fuel pellets vertically distributed by a suspending gas coolant flow (Harms and Fundamenski 1993). For the case of an incipient loss-of-coolant accident, the core discharges into a subcritical configuration with perpetual packed-bed cooling in a catchment by the most reliable of safety mechanisms: gravity.

The unique features associated with pellet discharge in a vertical column involves considerations beyond sedimentation (Maleki-Ardebili 1995) and conventional heat transfer investigations (Datta and Dalal 1995) in horizontal flows with low Reynolds numbers; these studies are commonly based on the Stokes approximation for the drag force, as employed, for instance, by Pedinotti *et al.* (1992), Datta and Dalal (1995), Mei *et al.* (1991). For the pellet suspension reactor concept, Harms and Kingdon (1993) showed that pellets falling with terminal velocities, have Reynolds numbers far beyond acceptability of the Stokes approximation. Indeed Reynolds numbers may reach values of 200 and more and it is therefore critical to find an appropriate model for description of the free particle motion (Maleki-Ardebili 1995).

In this work we report on the development of an approach to one feature of this fail-safe reactor concept namely the accidental discharge of the fuel pellets in the core. We define these dynamics by the following: the coolant pressure has dropped in such a way that the coolant is at rest or the coolant flow is slow enough to be laminar. In this case we establish a useful approximation for the drag force leading thereby to an analytical description of fuel pellets trajectories which can be effectively used in the computational simulation of pellet distributions, reducing the CPU time by several orders of magnitude, and allowing thereby the analysis of more realistic physical models of reactor cores. The laminarity assumption is important for this, but it represents only one and the simplest scenario of a loss-of-coolant accident. Furthermore, no experimental data of collision properties of fuel pellet shells and column walls have appeared and hence we have to accept the simplest assumptions: frictionless and energy conserving collisions. However, the results described below for these extreme simplifications seem to be quite acceptable for initial scoping assessments suggesting also that further analytical, computational, and experimental investigations need to be pursued.

The mean residence time of the pellet is of particular interest and is evaluated by averaging the data obtained for pellets with random initial conditions.

2. THE DRAG FORCE MODEL

Spherical pellets with diameter d and material density ρ_p move in the vertical column with height H and diameter D which is filled by a gas (e.g. helium) coolant characterized by a dynamic viscosity μ and density ρ_{cool}. A consistent set of the parameters above is listed in table 1 based on a scoping study of Harms and Kingdon (1993); we will label these parameters as "the scoping parameter set". The gravity and the pellet velocity define a plane, which will contain the drag force as well; therefore, for description of individual pellet trajectories the consideration can be restricted by two dimensions. We denote the position vector of the pellet and its components by $\mathbf{R} = (X, Z)$, time by T, and the velocity by $(d\mathbf{R}/dT) = \mathbf{V} = (V_x, V_z)$; here the X-axis is directed horizontally to the right, and Z-axis—vertically upward. Position and time are non-dimensionalized with pellet diameter d and the constant $\tau = \rho_{cool} d^2/\mu$, respectively, and, specifically, the dimensionless position $\mathbf{r} = (x, z) = \mathbf{R}/d$, time $t = T/\tau$, and velocity $\mathbf{v} = (v_x, v_z) = \mathbf{r} \equiv (d\mathbf{r}/dt) = R_r \mathbf{V}$, where $R_r = \tau/d = \rho_{cool} d/\mu$ (table 1). Commonly, the pellet Reynolds number is equal to $R_r|\mathbf{V}|$ and therefore $v \equiv |\mathbf{v}|$ is the Reynolds number. Due to the substantial difference between the fuel and coolant densities, we neglect the buoyancy, the added mass and inertia of the displaced gas terms in the equation of motion, as well as the Basset term so that the equation of motion is evidently

$$\dot{\mathbf{v}} = -\frac{3}{4} C_D \frac{\rho_{cool}}{\rho_p} v\mathbf{v} - R_r^2 \boldsymbol{g} d, \qquad [1]$$

where $\boldsymbol{g}$ is the gravitational acceleration, $g \equiv |\boldsymbol{g}| > 0$, and the drag coefficient, C_D, is assumed to depend only on the Reynolds number and is usually taken in the form like $\alpha/v + \beta v^{\gamma-2}$.

According to Clift *et al.* (1978), for the range $v < 800$, the best correspondence to experimental data is provided by $\alpha = 24$, $\beta = 3.6$ and $\gamma = 1.687$ with a tolerance of $\pm 5\%$. As will be shown later, in our case $v < v_{max} = 230$ and one may seek to find a simpler form of the $C_D(v)$ nonlinearity in order to treat the problem analytically. We note that for relatively small v values, details of the function $C_D(v)$ are not very important due to the multiplier $v\mathbf{v}$ in [1]. For the same reason, it seems to be more important to attend to the uncertainty of the function $C_{Dr} \equiv v^2 C_D = \alpha v + \beta v^\gamma$ rather than that of C_D. Evidently, the simplest form of nonlinearity—the binomial form $\tilde{C}_{Dr}(v, a_1, a_2) = a_1 v + a_2 v^2$—needs to be examined. In particular we employ the least squares criterion minimizing $\mathrm{Err} \equiv \int_0^{v_{max}} (C_{Dr} - \tilde{C}_{Dr})^2 \, dv$ by demanding $\partial \mathrm{Err}/\partial a_i = 0$. The latter leads to $\int_0^{v_{max}}$

Table 1. Scoping and derived parameters for the pellet–column system of interest

Category	Parameter	Value
Scoping	Coolant viscosity, μ (kg/m * s) (at $T = 600°C$)	4.06×10^{-5}
	Coolant density, ρ_{cool} (kg/m^3) (at $T = 600°C$)	2.75
	Pellet diameter, d (m)	5×10^{-4}
	Fuel (UC) density, ρ_p (kg/m^3)	13 630
	Column height, H (m)	5.0
	Column diameter, D (m)	0.2
	Pellet volume fraction, α	10%
Derived	$\tau = (\rho_{cool} d^2/\mu)$ (s)	0.017
	$R_r = (\rho_{cool} d/\mu)$ (s/m)	33.9
Dimensionless	v_{max}	230
	a_1	56.8
	a_2	0.522
	$A = \frac{3}{4}(\rho_{cool}/\rho_p)\, a_2$	7.90×10^{-5}
	$B = \frac{3}{8}(\rho_{cool}/\rho_p)\, a_1$	4.30×10^{-3}
	$C = (\rho_{cool}^2 g d^3/\mu^2)$	5.62
	$D_u = \sqrt{AC - B^2}$	0.206
	$D_d = 2\sqrt{AC + B^2}$	0.430
	v_{term}	218
	v_0	327

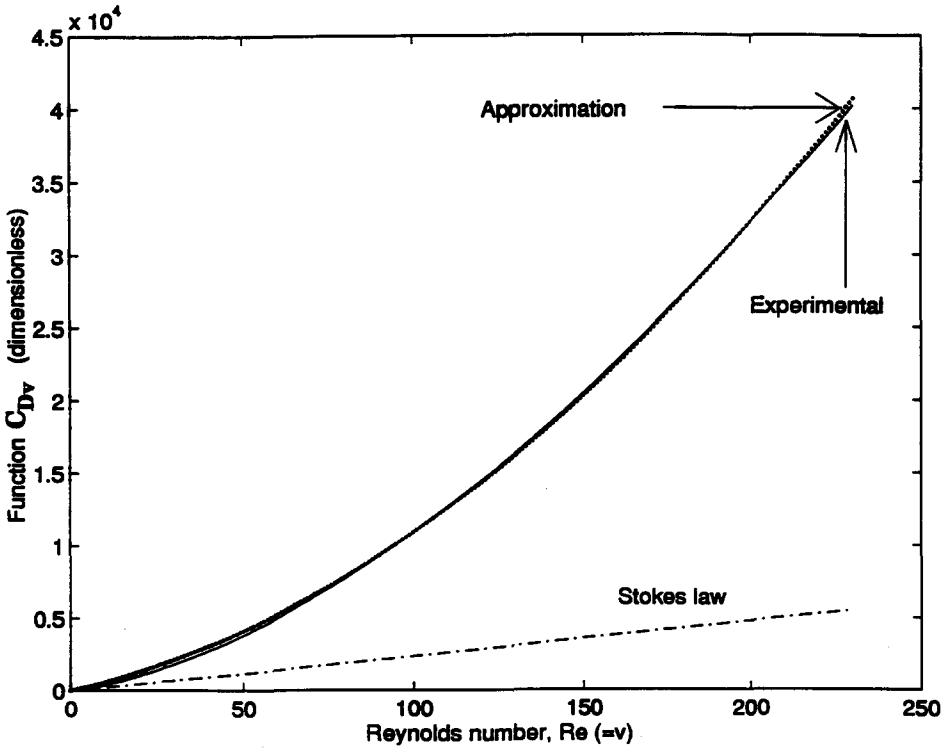

Figure 1. Experimentally determined function C_{Dv} (Clift *et al.* 1978) and approximation $\tilde{C}_{Dv}$ developed herein in comparison with Stokes law.

$(C_{Dv} - \tilde{C}_{Dv})v^i \, dv = 0$, $i = 1, 2$. The solution for a_1 and a_2 gives

$$a_1 = \alpha + 12\beta_{\max}^{\gamma-1}\left(\frac{4}{2+\gamma} - \frac{5}{3+\gamma}\right), \qquad [2]$$

$$a_2 = 20\beta v_{\max}^{\gamma-2}\left(\frac{4}{3+\gamma} - \frac{3}{2+\gamma}\right). \qquad [3]$$

Substitution of the $v_{\max}$ value and the scoping parameter set provides the values of a_1 and a_2, table 1. Figure 1 shows that the approximation $\tilde{C}_{Dv}$ obtained corresponds very well to C_{Dv} for the values of v giving the drag force comparable with the pellet weight; for the entire v range: $0 \leqslant v \leqslant v_{\max}$, the relative force error $\|\mathbf{F}| - |\tilde{\mathbf{F}}\|/mg$ does not exceed 1.2% and is less than the initial C_D approximation error; here $\tilde{\mathbf{F}}$ is the force calculated with $\tilde{C}_{Dv}$ instead of C_{Dv}.

The binomial approximation therefore is comparable to existing experimental functions, though it is not necessarily preferred for the description of experimental data. The advantage of this description can be understood from another point of view and will be expanded upon in the next chapter: its analytical simplicity allows one to obtain an analytical one-variable integral parametrization of pellet trajectories, providing thereby a powerful tool for effective computational simulations.

3. PELLET TRAJECTORIES

With the use of $\tilde{C}_{Dv} = a_1 v + a_2 v^2$, [1] can be written as

$$\dot{v}_x = -(Av + 2B)v_x, \qquad [4]$$

$$\dot{v}_z = -(Av + 2B)v_z - C, \qquad [5]$$

where $A = \frac{3}{4}\rho_{cool}a_2/\rho_p$, $B = \frac{3}{8}\rho_{cool}a_1/\rho_p$, and $C = R_v^2gd = \rho_{cool}^2gd^3/\mu^2$ for the scoping parameter set are listed in table 1.

The variables in [4] and [5] cannot be separated but some physical features of the problem of interest, in particular the oblong geometry, can help to simplify the equations. Normal operational suspension regime implies a coolant flow velocity comparable with the terminal velocity which is the maximum velocity of the falling pellet. Then, the order of magnitude of pellet velocity fluctuations is defined by the scale of turbulent fluctuations of the flow. For our conditions, this is less than 10% of the suspension velocity (Warsi 1993). Hence, we can expect that after stopping the coolant flow, the maximum of the pellet horizontal velocity will be approximately an order of magnitude less than the terminal velocity. When a falling pellet acquires the vertical velocity comparable with the terminal velocity, i.e. $v \sim v_{max}$, the v_x-dependent part in the expression $v = |v_z|\sqrt{1 + (v_x/v_z)^2}$ is negligible, typically not exceeding 0.5%, so that $v \approx |v_z|$. In the alternative case, when the pellet vertical velocity is comparable with the horizontal velocity, i.e. $|v_z| \sim |v_x| < 0.1 * v_{max}$, the total Reynolds number and, accordingly, the drag force are too small for us to be interested in details of the function $\tilde{C}_{Dv}(v)$ behaviour; in this case the substitution v by $|v_z|$ will not affect the pellet dynamics significantly. Thus in the entire range of v this variable in [4] and [5] can be substituted by $|v_z|$; having done that, [5] becomes independent of [4],

$$\dot{v}_z = -(A|v_z| + 2B)v_z - C, \tag{6}$$

and, after integration and substituting into [4], the latter can be further integrated as follows:

$$v_x = v_x(0)\,e^{-2Bt}\exp\left(-A\int_0^t |v_z(t)|\mathrm{d}t\right). \tag{7}$$

In order to solve [6], we have to consider a rising part of a trajectory: $v_z \geqslant 0$—in this case all variables and parameters will be supplied by the subscript "u"—and a falling part: $v_z < 0$—for which we will use the subscript "d". With this notation, we can separate [7] into two parts:

$$v_{xu} = v_{xu}(0)\exp\{-A[z_u(t) - z_u(0)] - 2Bt\}, \tag{8}$$

$$v_{xd} = v_{xd}(0)\exp\{A[z_d(t) - z_d(0)] - 2Bt\}. \tag{9}$$

We consider the rising part of the trajectory first.

3.1. *Rising trajectory*

Using the parameter $D_u \equiv \sqrt{AC - B^2}$ (table 1), we can write the solution of [6] for the rising trajectory as

$$v_{zu}(t) = \frac{1}{A}\{D_u \tan[(I_u - t)D_u] - B\}, \tag{10}$$

where the integration constant, I_u, is defined by

$$I_u = \frac{1}{D_u}\arctan P \tag{11}$$

with

$$P = \frac{1}{D_u}(Av_{zu}(0) + B) < P_{max} \equiv \frac{1}{D_u}(Av_{max} + B). \tag{12}$$

The time to maximum height, t_u, is defined by $v_{zu}(t_u) = 0$, yielding

$$t_u = I_u - \frac{1}{D_u}\arctan\frac{B}{D_u}. \tag{13}$$

Interestingly, regardless of the initial $v_z(0) > 0$, this time never exceeds the value $t_{umax} = \pi/2D_u$, or approximately 1.3 s for the scoping parameter set.

Integrating [10] we obtain

$$z_u(t) - z_u(0) = \frac{1}{A}\left[\ln\frac{\cos D_u(I_u - t)}{\cos D_u I_u} - Bt\right]. \qquad [14]$$

Since $0 \leqslant t \leqslant t_u$, we have $0 < \arctan(B/D_u) \leqslant D_u(I_u - t) < \arctan P_{max} < \pi/2$, so we need not take the absolute value for the logarithm argument. According to [11], we can replace $\cos D_u I_u$ by $1/\sqrt{1+P^2}$.

Analyzing a trajectory, it is necessary to check, for example, that the pellet has not reached the upper boundary of the column. For this, we have to be able to solve algebraic equations like $z_u(t) = \text{const}$, with respect to t. But the right hand part of [14] cannot be inverted to express $t = z_u^{-1}(z_u)$ through any known functions. For our purposes, we have to do extensive numerical calculations with a large number of pellets, and it is impossible to employ any numerical algorithm to invert [14] for any pellet with arbitrary initial state due to excessive CPU time consumption. Obviously the only way to be acceptable is to tabulate [14] with appropriate precision, and then, while inverting, to use a linear interpolation. But [14] depends on two variables: time, t, and, through I_u and P, on the initial value, $v_{zu}(0)$. The tabulation of this function will be demanding and limit the advantage of using analytically defined trajectories in comparison with direct numerical integration of the initial differential equations of pellet motion. To avoid this deficiency, we rewrite [14] in the form

$$z_u(t) = z_u(0) + \frac{1}{A}\left[\frac{1}{2}\ln(1+P^2) - BI_u\right] + \Phi_{zu}(D_u(I_u - t)), \qquad [15]$$

where the new function $\Phi(q)$ is defined by

$$\Phi_{zu}(q) = \frac{1}{A}\left(\ln\cos q + \frac{B}{D_u}q\right), \quad \arctan\frac{B}{D_u} \leqslant q < \arctan P_{max}. \qquad [16]$$

Thus, we have excluded the dependence on initial conditions in the function $\Phi_{zu}(q)$ and, for any parameter set, we need to tabulate this function of one variable only once prior to simulations. For the scoping parameter set, it is depicted in figure 2(a).

To determine the horizontal motion during rising, we substitute [14] into [8] to yield specifically

$$v_{xu}(t) = \frac{v_{xu}(0)\,e^{-Bt}}{\sqrt{1+P^2}\cos D_u(I_u - t)}. \qquad [17]$$

After integrating this equation we need to consider the choice, if possible, of functional expressions which—though complex—depend on only one variable. Following the necessary integrations and variable substitutions, we obtain

$$x_u(t) = x_u(0) + \frac{v_{xu}(0)\,e^{-BI_u}}{D_u\sqrt{1+P^2}}\left[\Phi_{xu}(D_u I_u) - \Phi_{xu}(D_u(I_u - t))\right], \qquad [18]$$

where

$$\Phi_{xu}(q) = \int_0^q \frac{\exp\frac{B}{D_u}q}{\cos q}\,dq, \quad \arctan\frac{B}{D_u} \leqslant q < \arctan P_{max}. \qquad [19]$$

The tabulation of this function, from the numerical point of view, is not much harder than in the previous case. The result for the scoping parameter set is depicted in figure 2(b).

Having the solutions in forms [15] and [18] and taking into account the monotonic character of [16] and [19], we can formulate a simple and fast algorithm (e.g. dichotomic) for finding the time of pellet collision with any plane $Lx + Mz + N = 0$, where L, M, N are constants; in addition, we can also consider collision even with another pellet which has different values of $v_{zu}(0)$, $v_{xu}(0)$, I_u, and P, in [15] and [18].

3.2. *Falling trajectory*

For the alternative case $v_z < 0$, we introduce the parameters $D_d = 2\sqrt{AC + B^2}$, $v_{term} = (D_d - 2B)/2A$, and $v_0 = (D_d + 2B)/2A$ (table 1). These parameters obey the equality: $Av_{zd}^2 - 2Bv_{zd} - C = A(v_{zd} + v_{term})(v_{zd} - v_0)$. Hence, the solution of [6] can be written as

$$v_{zd}(t) = \frac{-v_{term} + v_0 I_d \, e^{-D_d t}}{1 + I_d e^{-D_d t}} \qquad [20]$$

with the integration constant given by

$$I_d = \frac{v_{term} + v_{zd}(0)}{v_0 - v_{zd}(0)} < 1. \qquad [21]$$

The limit $\lim_{t\to\infty} v_{zd}(t) = -v_{term}$ can be called "the terminal Reynolds number"; for the scoping parameter set its absolute value is approximately 218, corresponding to the terminal velocity $V_{term} = v_{term}/R_v \approx 6.4$ m/s.

Integration of [20] yields

$$z_d(t) = z_d(0) - v_{term} t - \frac{1}{A} \ln \frac{1 + I_d \, e^{-D_d t}}{1 + I_d}. \qquad [22]$$

One typical particular situation is interesting: if initially a pellet rises, then a falling trajectory will start with $v_{zd}(0) = 0$; in this case then

$$v_{zd}(t) = -v_{term} \frac{1 - e^{-D_d t}}{1 + \frac{v_{term}}{v_0} e^{-D_d t}}, \qquad [23]$$

$$z_d(t) = z_d(0) - v_{term} t - \frac{1}{A} \ln \frac{v_0 + v_{term} \, e^{-D_d t}}{v_0 + v_{term}}. \qquad [24]$$

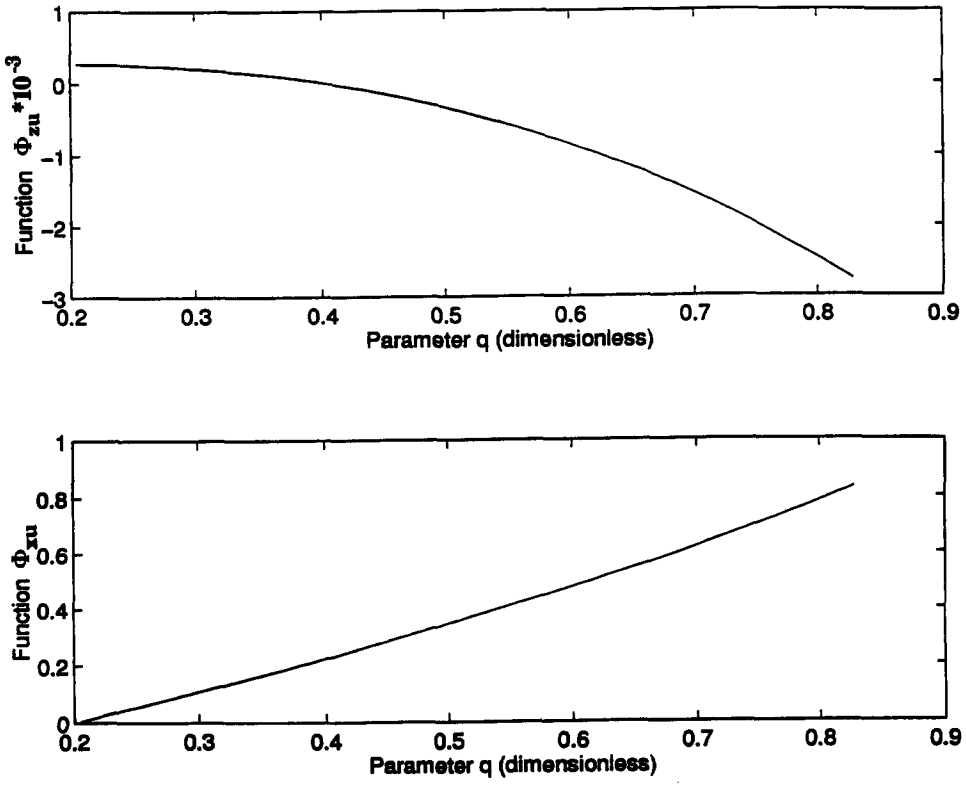

Figure 2. Dimensionless functions $\Phi_{zu}(q)$ and $\Phi_{vu}(q)$ used for rising trajectory description.

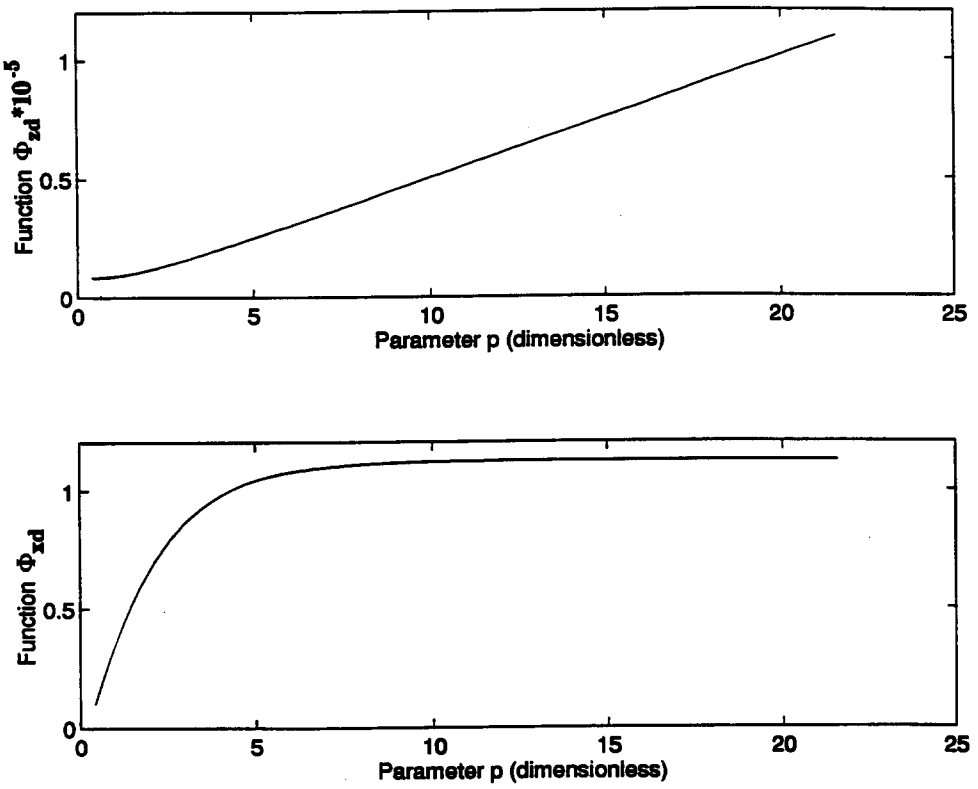

Figure 3. Dimensionless functions $\Phi_{zd}(p)$ and $\Phi_{xd}(p)$ used for falling trajectory description.

For the scoping parameter set a pellet will obtain 50% of the terminal velocity approximately in 0.4 s proceeding a distance approximately 0.7 m.

To determine the time range for [22], we need to estimate the maximum time, t_{dmax}, of pellet falling in the column with height H—a nominal value is $H = 5$ m (Harms and Kingdon 1993)—by solving the equation $z_d(t_{dmax}) = 0$ with initial conditions: $v_{zd}(0) = 0$, $z_d(0) = H/d$. For the scoping parameter set the numerical solution gives $t_{dmax} = 74$ or 1.25 s.

As for the previous subsection, we have to transform this equation to reduce it to a transcendental function of one variable. To do this, we define the constant $t_0 = -(1/D_d)\ln I_d > 0$ and obtain

$$z_d(t) = z_d(0) + v_{term}t_0 + \frac{1}{A}\ln(1 + I_d) - \Phi_{zd}(D_d(t_0 + t)), \qquad [25]$$

where the function to be tabulated is given by

$$\Phi_{zd}(p) = \frac{1}{A}\ln(1 + e^{-p}) + \frac{v_{term}}{D_d}p, \quad D_d t_{0min} \leqslant p < D_d(t_{0max} + t_{dmax}) \qquad [26]$$

and displayed in figure 3(a). Here $t_{0min} = (1/D_d)\ln(v_0/v_{term})$ and $t_{0max} = -(1/D_d)\ln\epsilon$, where ϵ is the least CPU nonzero number, i.e. the least ϵ such that $1 + \epsilon \neq 1$. For the scoping parameter set and ordinary precision ($\epsilon \sim 1e - 7$), which seems to be quite acceptable, $t_{0min} \approx 9$ and $t_{0max} \approx 375$, or 6.4 s.

Further, [22] and [9] yield the formula for v_{xd} as

$$v_{xd}(t) = \frac{v_{xd}(0)(1 + I_d)\,e^{-(Av_{term} + 2B)t}}{1 + I_d\,e^{-D_d t}}, \qquad [27]$$

which upon integration provides specifically

$$x_d(t) = x_d(0) + \frac{v_{term}(1 + I_d)\, e^{(Av_{term} + 2B)t_0}}{D_d}[\Phi_{xd}(D_d(t_0 + t)) - \Phi_{xd}(D_d t_0)], \quad [28]$$

where

$$\Phi_{xd}(p) = \int_0^p \frac{\exp\left(-\frac{Av_{term} + 2B}{D_d} p\right)}{1 + \exp(-p)}\, dp, \quad D_d t_{0min} \leqslant p < D_d(t_{0max} + t_{dmax}). \quad [29]$$

This function is depicted in figure 3(b).

4. COMPUTATIONAL SIMULATION

The derived expressions for $x_u(t)$, $z_u(t)$ and $x_d(t)$, $z_d(t)$, together with four universal Φ-functions [19], [16], [29] and [26]—which are independent of initial conditions—allow the determination of points and times of pellet collisions with the column walls and with each other by the dichotomic search through the tables containing the values of the Φ-functions.

In order to investigate statistical properties of the pellet community, we judge that the direct tracing of pellet trajectories, frequently called the "molecular dynamics" methods (Hoover 1986), appears to be the most appropriate technique. The compromise between computational restrictions and representativity of simulations requires the choosing of a reasonable number of pellets in a simulation, e.g. $N \sim 10^3$ and is subject to one of the alternatives:

(a) to study the collision mechanism influence of pellet dynamics, we have to sustain the pellet volume fraction rather than the pellet diameter; that will cause a change in the column diameter—pellet diameter ratio from 400 to approximately 20, or

(b) to realistically describe the drag force, the pellet diameter is the main parameter and, hence, should be taken from table 1; this will significantly lower the pellet volume fraction.

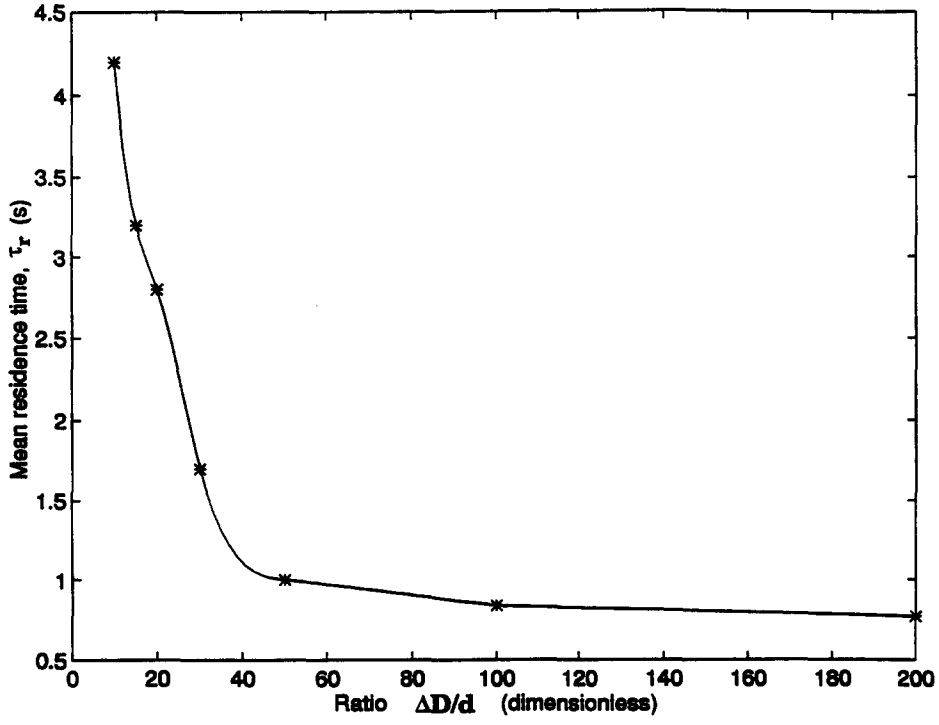

Figure 4. Spline interpolation for the pellet mean residence time, τ_r, as a function of the ratio $\Delta D/d$, where ΔD is the lower end gap and d is the pellet diameter.

Simulations of the pellet dynamics with the use of the technique developed by Kornilovsky *et al.* (1995), in an empty (vacuum) column with the dimensions according to table 1 and column diameter–pellet diameter ratio equal 20, for $N = 1000$ pellets, have shown that about 80% collisions are of the pellet–pellet type. In the case under investigation here, and seeking to describe realistically the drag force, we have to take the column diameter–pellet diameter ratio to be equal to 400 according to table 1. Simulations in the empty column demonstrate that pellet–pellet collisions are rare—only approximately 17% of all collisions for the same number of pellets. For this a reason exists to expect that mutual collisions are not very important factors in affecting the mean time of pellet residence in the column. Based on this assumption then we consider the case when mutual collisions can be neglected. In this case it is sufficient to model collisions of one pellet with the column walls to determine the most interesting parameters of pellet dynamics—the time to escape through the low open end of the column, that is the pellet residence time. As the lower open end of the column needs to be narrowed in order to avoid pellet loss in the normal suspension regime (Harms and Fundamenski 1993), we model this end to be of the cone shape with the lower gap to be chosen. We then take a pellet with initial conditions randomly chosen from the uniform distribution and trace the pellet trajectory until it leaves the column; the number of repetitions is chosen until stable estimate for the mean residence time τ_r is obtained by averaging.

For our computational simulation, we take the height of the cone part to be equal to $0.1 * H$, and vary the gap in the range $10d$–$200d$. Experiments suggest that in order to arrive at a stationary estimate for mean residence time, averaging data for 100 pellets' escapes appears sufficient. The result is depicted in figure 4 and shows that this escape time is approximately constant and less than 1 s if the gap width exceeds $50d = D/8$.

5. SUMMARY AND CONCLUSION

Critical to the determination of non-equilibrium micro-pellet dynamics in gas-filled vertical columns is the description of the drag force. The approximation we have here developed appears in excellent agreement with experiment and generally well suited for analytical purposes. Of further importance is the selective application of molecular dynamics considerations rendering thereby a difficult problem tractable. For the case of interest, pellet-pellet collisions are rare, obviating the need to trace simultaneous motion of pellets, but the approach undertaken here permits its ready extensions to a denser pellet gas. A useful and effective methodology for a class of complex non-equilibrium problems is thus established.

In general, the parametrization developed herein can be employed for effective examination of a wide class of problems dealing with particle dynamics in gas-filled vertical columns, including evaluations of importance to the development of pellet suspension nuclear reactor cores.

Acknowledgement—Financial support for the research reported upon herein has been provided by the Natural Sciences and Engineering Research Council of Canada.

REFERENCES

Clift, R., Grace, J. R. and Weber, M. E. (1978) *Bubbles, Drops and Particles*. Academic Press, New York.

Datta, N. and Dalal, D. C. (1995) Pulsatile flow and heat transfer of a dusty fluid through an infinitely long annular pipe. *Int. J. Multiphase Flow* **21**, 515–528.

Harms, A. A. and Fundamenski, W. R. (1993) Fail-safe decay-heat removal in a pellet suspension fission reactor, *Proc. Seventh Int. Conf. Emerging Nuclear Energy Systems*, Chiba, Japan, 20–24 September.

Harms, A. A. and Kingdon, D. R. (1993) Passively fail-safe fission reactor based on pellet suspension technology, *Proc. Int. Joint Power Generation Conf.*, Kansas City, MO, USA, 17–21 October.

Hoover, W. G. (1986) *Molecular Dynamics*. Springer, Berlin.

Kaftori, D., Hetsroni, G. and Banerjee, S. (1995) Particle behavior in the turbulent boundary layer. I. Motion, deposition, and entrainment. *Phys. Fluids* **7**, 1095–1106.

Kornilovsky, A. N., Kingdon, D. R. and Harms, A. A. (1996) On the dynamics of fuel pellets in suspension. *Ann. Nucl. Energy* **23,** 171–182.

Maleki-Ardebili, M. (1995) Sedimentation of a cylindrical particle in an oscillating fluid. *Int. J. Multiphase Flow* **21,** 285–303.

Mei, R., Lawrence, C. J. and Adrian, R. J. (1991) Unsteady drag on a sphere at finite Reynolds number with small fluctuations in the free-stream velocity. *J. Fluid Mech.* **233,** 613–631.

Pedinotti, S., Marotti, G. and Banerjee, S. (1992) Direct numerical simulation of particle behaviour in the wall region of turbulent flows in horizontal channels. *Int. J. Multiphase Flow* **18,** 927–941.

Warsi, Z. U. A. (1993) *Fluid Dynamics: Theoretical and Computational Approaches*. CRC Press, Boca Raton, FL.